Contents list available at CBIORE journal website

International Journal of Renewable Energy Development

Journal homepage: https://ijred.cbiore.id

Research Article

Techno-economic evaluation of optimization and rule-based energy management for grid-tied PV-BESS prosumers

Hideki Kakhai[a], Thipwan Fangsuwannarak[a*], Jirut Rhianprayoon[b], Vijittra Saengpredekorn[c]

[a]*School of Electrical Engineering, Institute of Engineering, Suranaree University of Technology, Nakhon Ratchasima, 30000, Thailand.*

[b]*Energy Solution Business, Nuovo Plus Co., Ltd., Chatuchak, Bangkok 10900, Thailand.*

[c]*Getz Energy Co.,Ltd., Chatuchak, Bangkok 10900, Thailand.*

Abstract.This research investigates the techno-economic feasibility of an energy management system (EMS) for a grid-tied photovoltaic-battery energy storage system (PV-BESS) prosumer at a university campus. The study introduces an advanced Optimization-Based Control (OBC) framework, comparing Particle Swarm Optimization (PSO) and Genetic Algorithms (GA) against conventional Rule-Based Control (RBC). A primary contribution is the systematic simultaneous parameter-tuning framework, utilizing a grid-search methodology with 30 independent simulations per configuration to ensure statistically reliable BESS scheduling. Results demonstrate that OBC-PSO and OBC-GA achieved annual net profit improvements of 13.50% and 11.72%, respectively, by effectively leveraging Time-of-Use (TOU) arbitrage. Furthermore, precise optimization significantly mitigated battery degradation, extending the replacement cycle from 8 to 10 years and drastically reducing long-term capital expenditure. A 25-year lifecycle analysis reveals that OBC-PSO attains a maximum Net Present Value (NPV) of 97,639 USD, representing a 98.57% improvement over RBC, while reducing the discounted payback period from 11.71 to 6.74 years. The Levelized Cost of Energy (LCOE) was also reduced from 0.085 to 0.078 USD/kWh. Sensitivity analysis confirms that the proposed tuning-centric OBC approach provides a robust financial buffer against electricity price volatility and BESS cost fluctuations. These findings underscore that rigorous algorithm configuration and initialization are essential for enhancing the commercial viability and reliability of grid-tied prosumer systems in modern smart cities.

Keywords: Techno-economic analysis, Energy management, Prosumer, Photovoltaic-battery system, Optimize algorithm

@ The author(s). Published by CBIORE. This is an open access article under the CC BY-SA license (https://creativecommons.org/licenses/by-sa/4.0/).

Received: 21st January 2026; Revised 17th Sept 2026; Accepted: 25th Oct 2026; Available online: 1st Nov 2026

1. Introduction

In the modern energy landscape, the roles of producers, consumers, and prosumers are undergoing a significant transformation. Prosumers, entities that both generate and consume electricity via their own Renewable Energy Sources (RES), have become critical participants in decentralized energy markets. By balancing local supply and demand, prosumers can reduce reliance on centralized power generation and mitigate rising electricity costs (Zafar *et al.,* 2018; Patrizi *et al.,* 2022).

However, the high penetration of variable RES, such as solar and wind, introduces substantial uncertainty and volatility into the power grid, threatening the stability and reliability of electrical systems (Wynn *et al.,* 2023). Battery Energy Storage Systems (BESS) have emerged as a pivotal solution to these challenges. They effectively mitigate the intermittency of renewable generation, enhance power quality, and provide critical grid services, including frequency regulation, peak shaving, and energy time-shifting (Njoka *et al.,* 2025; Hadjipaschalis *et al.,* 2009). University campuses, characterized by extensive infrastructure, high energy demand, and available rooftop space, serve as ideal environments for investigating these innovative smart community models. Consequently, numerous studies have explored the techno-economic feasibility of PV-BESS deployment within campus settings to optimize both environmental and financial outcomes. (Zhou *et al.,* 2025)

A comprehensive techno-economic analysis must integrate technical performance, such as BESS degradation models and operational efficiencies, with financial metrics like Net Present Value (NPV) and internal rate of return (IRR). Such evaluations are essential for promoting the cost-effective adoption of these systems (Mohamed *et al.,* 2021; Khan *et al.,* 2022). The effectiveness of a BESS depends largely on the Energy Management System (EMS), which schedules charging and discharging cycles. While Rule-Based Control (RBC) remains popular due to its simplicity and real-time responsiveness, its reliance on fixed, heuristic decisions often limits its ability to achieve global cost-optimality in complex market scenarios (Abdul Basit *et al.,* 2022; Pippia *et al.,* 2019). Controlling the operation of BESS requires energy management systems (EMS) to ensure optimal and efficient energy utilization across various operating conditions. Energy management strategy as an energy arbitrage focuses on storing surplus energy from RES into BESS, not only to mitigate reliance on the main power grid but also to generate revenue from overproduction. The modern hybrid energy market, using optimized operation scheduling of BESS and optimal energy allocation, provides significantly

* Corresponding author
Email: thipwan@g.sut.ac.th (T. Fangsuwannarak)

https://doi.org/10.61435/ijred.2026.62267
ISSN: 2252-4940/© 2026.The Author(s). Published by CBIORE

enhanced benefits for energy transactions and auction mechanisms compared to traditional energy trading on the main grid (Zhang *et al.,* 2021). Although the integration of RES with BESS into the grid inevitably increases operational costs, it offers greater consumer convenience. Unlike demand side management (DSM) strategies, which require alterations in daily routines to alleviate electricity expenses, this approach preserves existing consumption patterns while still improving economic outcomes. Consequently, BESS emerges as a promising and compelling solution for energy management in power systems with a high penetration of RES.

The simplicity and real-time responsiveness of Rule-Based Control (RBC) make it a widely adopted strategy for Energy Management Systems (EMS) in BESS applications. Conventional grid-connected PV systems frequently utilize RBC to mitigate electricity costs and maintain operational stability with minimal processing requirements (Abdul Basit *et al.,* 2022; Behzadi & Sadrizadeh, 2023; Pan *et al.,* 2021). While RBC schemes have demonstrated overall operational efficiency in hybrid microgrids (Pippia *et al.,* 2019), their reliance on predefined heuristics limits their capacity to provide globally optimal solutions in highly dynamic or complex environments.

In contrast, Optimization-Based Control (OBC) offers a mathematically rigorous framework that employs advanced optimization techniques to achieve high scheduling precision and system flexibility. OBC-driven hybrid renewable microgrids have shown substantial improvements in energy efficiency under varying weather conditions, including both clear and partly cloudy days (Mquqwana *et al.,* 2024; Luo *et al.,* 2020). Furthermore, the efficacy of OBC in reducing total operational expenses and minimizing power plant costs has been well-documented (Adenuga *et al.,* 2023). However, the real-time deployment of OBC in large-scale or non-linear hybrid systems is often hindered by a significant computational burden and inherent scalability challenges (Khan *et al.,* 2025). The complexity is further compounded by system dynamicity, which necessitates sophisticated controller design and intensive parameter tuning to avoid local optima (Çınar *et al.,* 2021; Shadaei *et al.,* 2020; Fadil *et al.,* 2020). Despite these advancements, the systematic and simultaneous tuning of multiple optimization parameters to maximize the economic performance of RE systems for prosumers remains underexplored. Thus, for grid-tied prosumers, maximizing techno-economic benefits are investigated in this study by scheduling BESS based on its efficiency decline, which is a notable challenge. The many research exploited the modelled sites for demonstrating improved OBC strategies, but in this study, a real-world prosumer environment is demonstrated to identify the most effective strategy for increasing revenues.

Recent research into transactive energy management has demonstrated that certain metaheuristic algorithms, such as the Slime Mould Algorithm (SMA), can offer faster convergence and reduced parameter-tuning complexity compared to traditional methods like Particle Swarm Optimization (PSO) and Genetic Algorithms (GA) (Gbadega *et al.,* 2025). Recent literature suggests that the dynamic adjustment of population-based parameters in metaheuristic algorithms offers substantial economic advantages over static configurations. Specifically, evidence indicates that GA can achieve lower operational expenditures than PSO under certain microgrid architectures, highlighting the importance of algorithm selection (Mouna *et al.,* 2025). Battery decline due to more frequent charging and discharging can result in a reduction of its maximum capacity. This dynamic battery degradation can directly be considered in the objective function for IEMS (Integrated energy management system) improvement (*Yousri et al., 2023*). Battery degradation modeling and lifecycle analysis, critical for understanding the non-linear aging of batteries in prosumer systems, have not been extensively explored in various EMS strategies (*Sharma et al., 2024*). Evaluating and analysing the performance across improved EMS control strategies in prosumer applications, while incorporating the non-linear nature of battery degradation and its replacement, remains a challenging task. Thus, this paper addresses this gap by proposing an optimal BESS scheduling framework that incorporates a new systematic with some significant tuning parameters to approach both PSO and GA.

A real-world grid-tied PV-BESS prosumer system at Suranaree University of Technology (SUT), Thailand is used as a case study to rigorously evaluate the proposed Optimization-Based Control (OBC) strategies against a conventional Rule-Based Control (RBC) strategy through numerical simulation.

The main goal of this study is to connect the theoretical aspect of energy management with the real economic conditions of prosumer-sized PV-BESS systems. To achieve this, the study pursues the following specific aims:

- A Systematic Tuning Framework for enhanced EMS: Development of a simultaneous parameter-tuning methodology using a grid-search approach with 30 independent simulations for each configuration to ensure statistically reliable initialization for BESS scheduling.
- A Comparative Evaluation of Techno-Economic Performance: A detailed techno-economic comparison of OBC-PSO, OBC-GA, and RBC strategies within a real-world prosumer environment to identify the most effective strategy for maximizing energy trading profits.
- An Analysis of Lifespan and Sensitivity of BESS: A comprehensive 25-year economic assessment that incorporates battery degradation and replacement costs and sensitivity tests for BESS cost reductions and electricity tariff volatility.

2. Methodology: System Site Description and Experimental Implementation

2.1 Prosumer Based Grid-tied PV-BESS System

Suranaree University of Technology (SUT) is used as an innovative smart city model to explore techno-economic evaluation of optimization and rule-based energy management for grid-tied PV-BESS prosumer model. The study investigates the functioning of Student Dormitory S5 as a grid-connected prosumer system positioned on the university campus, utilizing the 5.997 MW grid-tied PV system. The S5 prosumer installation comprises a 138.24 kWp photovoltaic (PV) array, consisting of 256 modules distributed across three orientations to capture solar irradiance effectively throughout the day. This array is integrated with a 100 kW/227.2 kWh BESS and a 100 kW smart inverter. The system is coupled to the campus 22 kV distribution network, which connects various prosumers with a total of 1.59

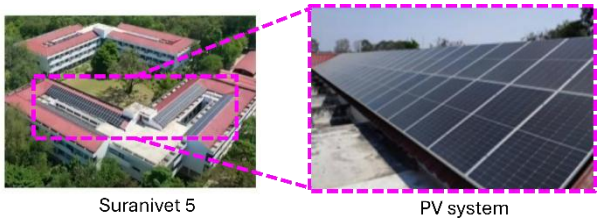


Fig 1. PV rooftop of 138.24 kWp at the S5-prosumer

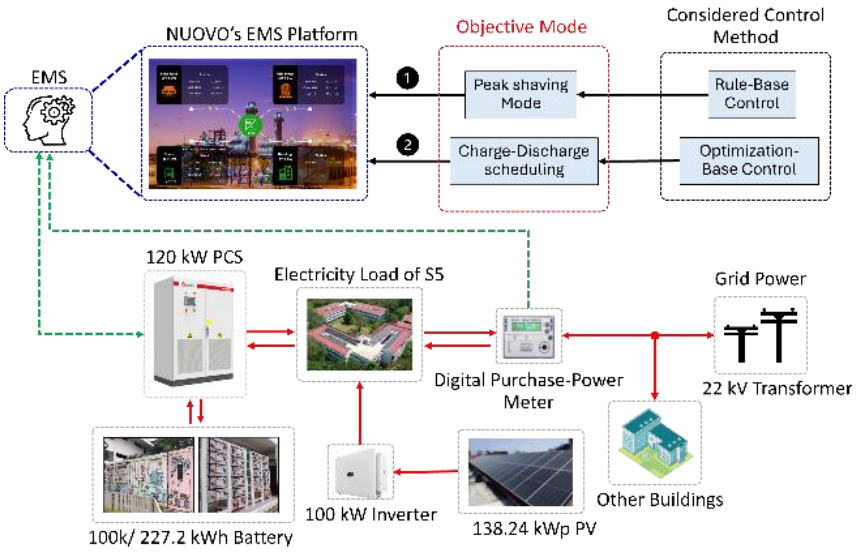


Fig 2. Schematic representation of the grid-tied PV-BESS of S5-prosumer

MW PV, one 4.27 MW floating PV, and consumer groups via a 115 kV substation.

The experimental site is located in Thailand at geospatial coordinates 14°53′51.29″ N and 102°0′49.68″ E. For this study, longitudinal PV generation data were collected over a one-year period through direct measurements from the smart inverter. To ensure high data integrity for the subsequent techno-economic analysis, these records were retrieved from a dedicated database platform established and maintained by the NUOVO team.

2.2 Component and Functions of BESS in Grid-Tied PV-BESS

The schematic configuration of the grid-tied PV-BESS is illustrated in Figure 2. The system comprises a 100 kW/227.2 kWh battery pack integrated with a dedicated Battery Management System (BMS), an Energy Management System (EMS), and a 120 kW power conditioning system (PCS).

As a critical component of the architecture, the bidirectional PCS facilitates the conversion of DC from the BESS to AC for local loads and grid export, while also rectifying grid AC for battery charging. It ensures robust grid synchronization by aligning voltage, frequency, and phase parameters to maintain power quality and stability. Furthermore, the PCS manages the energy exchange between the PV-BESS and the utility grid, optimizing storage and export intervals. To enhance system resilience, safety features such as anti-islanding protection are integrated to ensure rapid disconnection during fault conditions or grid outages.

The EMS is currently detecting grid power through the S5 smart meter. The EMS serves as the primary platform for monitoring and control, maintaining the balance between PV generation and prosumer consumption. As depicted in Figure 3, each battery module is equipped with a BMS that transmits operational data to the Battery Array Management System (BAMS) via CAN bus communication. The EMS subsequently retrieves this aggregated information and issues dispatch instructions to the PCS through the Modbus RTU protocol. Additionally, real-time measurements from the smart meter and PV inverter are acquired via Modbus TCP. This data is relayed to a cloud-based platform for remote monitoring, with grid power detection performed continuously through the S5 smart meter.

To optimize energy management performance and attain specific economic objectives, the EMS for the prosumer can be configured with BESS scheduling strategies based on either RBC or OBC. As illustrated in Figure 4, a real-time data dashboard developed by the NUOVO team facilitates the continuous monitoring of system parameters and the management of energy settings. The implementation of optimization strategies, coupled with simultaneous parameter tuning via the EMS controller, represents a novel approach to achieving superior techno-economic energy management for the prosumer.

This study utilizes a simulation model based on the technical characteristics of semi-solid-state lithium-iron phosphate (LFP) battery technology, a joint venture development between 24M and GPSC. This LFP chemistry is distinguished by its high power and energy density, as well as an extended operational lifespan. The BESS, which possesses a rated capacity of 100 kW / 227.2 kWh (Figure 3), comprises 40 individual modules, each

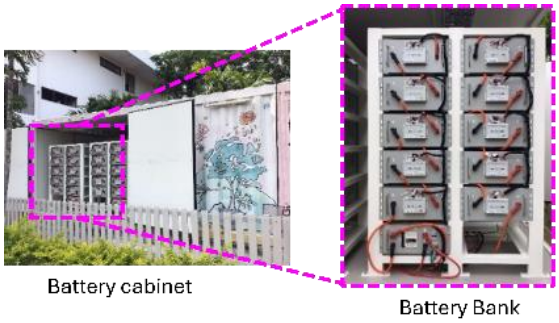


Fig 3. BESS capacity of 100 kW/227.2 kWh installed at S5 prosumer

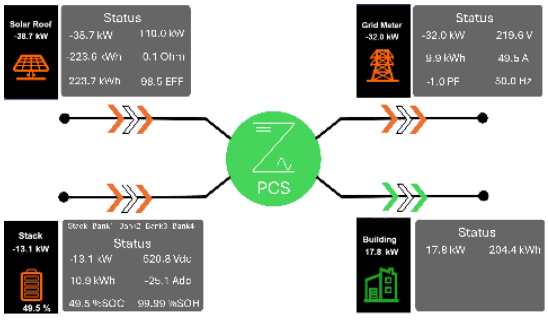


Fig 4. The NUOVO platform created in this study

with a capacity of 5.68 kWh and a 0.3 C-rate. These modules are configured into four distinct banks, with each bank containing 10 modules connected in series and regulated by a dedicated Battery Control Management Unit (BCMU).

The battery parameter SoC represents the amount of energy stored in the battery, as shown in Equation (1).

$$SoC(t) = SoC(t-1) + P_B^{CHG}(t) \cdot \eta_{CHG} \cdot \eta_{BAT} \cdot \Delta t - P_B^{DIS}(t) \cdot \frac{1}{\eta_{BAT}\eta_{DIS}} \cdot \Delta t \quad (1)$$

where P_B^{CHG} and P_B^{DIS} represent the charging and discharging power of the battery, respectively. η_{CHG}= 80% and η_{CHG}= 90%, they represent the charging and discharging efficiency of the PCS, respectively, while η_{BAT} of 98% is denotes the efficiency of the battery module.

The EMS architecture (Figure 4) provides a robust framework for effective system oversight, allowing for the external scheduling of BESS operations. It maintains real-time data acquisition for load profiles, PV output, and net grid interaction, while simultaneously monitoring internal battery metrics including SoC, SoH, voltage, and current.

2.3 Strategy models for EMS Control

2.3.1 Strategy of Rule-Based Control

RBC serves as a basic operational component of the EMS in this study. The primary function of the RBC mechanism is to minimize net grid power by maintaining a balance between local PV generation and power demand. Under this strategy, the power setpoint (P_{SET}) is defined as zero kW. The instantaneous net grid power ($P_{Grid}^{NET}(t)$), as detected by the smart meter, is defined such that positive values indicate grid power consumption (import) and negative values indicate surplus power (export).

The RBC logic operates over a continuous time series (T) of 168 hours (7 days) with hourly scheduling updates. As illustrated in the flow diagram in Figure 5, the system continuously monitors the net grid power and the battery SoC to determine whether to charge, discharge, or remain idle.

- Idle State: The battery remains non-operational if the $SoC(t)$ is outside the predefined operational bounds (SoC_{min} - SoC_{max}) or if the net grid power already matches the setpoint ($P_{Grid}^{NET}(t) = P_{SET}$).
- Charging Logic: If the measured $P_{Grid}^{NET}(t) < P_{SET}$, (indicating surplus generation), the EMS verifies the current $SoC(t)$. If $SoC(t) < SoC_{max}$, the BESS is charged by the excess power, where $P_B(t) = P_{SET} - P_{Grid}^{NET}(t)$.
- Discharging Logic: If $P_{Grid}^{NET}(t) > P_{SET}$ (indicating a load power demand), the EMS checks if $SoC(t) > SoC_{min}$. If this condition is met, the battery discharges to cover the load, with the discharge power defined as $P_B = P_{Grid}^{NET}(t) - P_{SET}$.

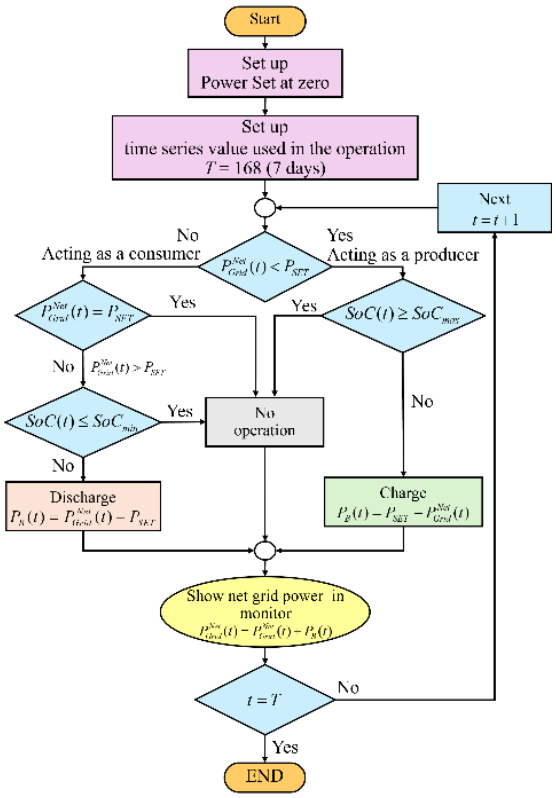


Fig 5. The diagram of the RBC operation mechanism to control BESS

This iterative monitoring and control process repeats hourly until the end of the simulation period (T). A comprehensive summary of the operational conditions managed by the RBC mechanism is provided in Table 1.

2.3.2 A novel approach of simultaneous parameter tuning in OBC

The seasonal net profit (NP), which includes savings from excess energy sales, as described in Equation (2), is calculated.

$$NP = (C_{purchase}^{No\ PV_BESS} - C_{purchase}^{PV_BESS}) + C_{selling}^{PV_BESS} \quad (2)$$

where NP is the net profit of PV-BESS prosumer. $C_{purchase}^{PV_BESS}$ and $C_{purchase}^{No\ PV_BESS}$ are the total expense of electricity acquisition, considering with and without PV-BESS, respectively. $C_{selling}^{PV_BESS}$ is a negative value from the $P_{Grid}^{NET}(t)$ term, representing the cost of revenue from selling electricity to other buildings.

The OBC strategy is designed to maximize the net profit of prosumer by optimizing the hourly charge-discharge scheduling of the BESS in response to Time-of-Use (TOU) tariffs. In this peer-to-peer (P2P) energy trading setup, surplus energy exported by S5 prosumer is given priority for sale to other

Table 1
Details of the BESS conditions under the RBC mechanism in the prosumer system.

Conditions	Battery status	Battery operation
$P_{Grid}^{NET}(t) = P_{SET}$	Idle State	Due to the presence of the power balancing
$P_{Grid}^{NET}(t) > P_{SET}$ and $SoC(t) < SoC_{min}$	Idle State	Battery capacity is not enough for the stability operation
$P_{Grid}^{NET}(t) > P_{SET}$ and $SoC(t) > SoC_{max}$	Idle State	The battery capacity is already full.
$P_{Grid}^{NET}(t) < P_{SET}$ and $SoC(t) < SoC_{max}$	Charging	Energy stored into the battery
$P_{Grid}^{NET}(t) > P_{SET}$ and $SoC(t) > SoC_{min}$	Discharging	Discharge energy from the battery

Table 2
TOU tariff rates in this study.

Parameter	Time period	Price	Unit
Energy charge	On-peak (10:00-22:00)	0.12	USD/kWh
	Off-peak (22:00-10:00)	0.079	
Peak demand charge	On-peak (10:00-22:00)	2.26	USD/kW
	Off-peak (22:00-10:00)	-	

demand-side nodes within the SUT grid network. The optimization problem is formulated to minimize total operational costs (thereby maximizing net profit), as defined by the objective function in Equation (3):

$$\boldsymbol{C_{NP}} = \sum_{t=1}^{T} C_E(t) P_{Grid}^{Net}(t) + C_P P_{Peak} + C_{Ft} \sum_{t=1}^{T} P_{Grid}^{Net}(t) \quad (3)$$

where C_{NP} is an objective value representing the summation of purchasing energy cost and selling energy cost. A positive C_{NP} value indicates that grid-import expenditures surpass export revenues. Conversely, a negative C_{NP} reflects a net financial gain, occurring when surplus energy sales exceed the cost of grid-purchased power. $C_E(t)$ represents the energy expense at time t according to the Time of Use (TOU) tariff system in Thailand. C_P is the cost of peak power demand at on-peak times. C_{Ft} is the cost of the fuel tariff charge. The net grid power flow, $P_{Grid}^{Net}(t)$, for the S5 building represents a bidirectional variable; positive values denote net power consumption from the grid, whereas negative values indicate net power export to the utility.

The detailed TOU pricing scheme, which is used in economic analysis, is illustrated in Table 2. The P2P energy trading model utilizes the transaction rate based on a TOU tariff structure.

The constraint Equation (4)-(7) is illustrated as:

$$P_{Grid}^{Net}(t) = \sum_{t=1}^{T} P_L(t) + P_{PV}(t) + P_B(t) \ \ for\ t\ =\ 1, 2, 3, \dots T \quad (4)$$

where $P_L(t)$, $P_{PV}(t)$ and $P_B(t)$ are the S5 load power, the PV power and BESS power at time t, respectively.

$$SoC_{min} \le SoC(t) \le SoC_{max} \quad (5)$$

$$P_B^{min} \le P_B(t) \le P_B^{max} \quad (6)$$

$$P_{Grid}^{Net}(min) \le P_{Grid}^{Net}(t) \le P_{Grid}^{Net}(max) \quad (7)$$

where $SoC(t)$ is the state of charge of the BESS capacity at time t. SoC_{min} is the state of charge at the minimum set level. SoC_{max} is the state of charge at the maximum set level. $P_B(t)$ is BESS power at the time t. P_B^{min} is battery power at the minimum set level. P_B^{max} is battery power at the maximum set level. $P_{Grid}^{Net}(min)$ is net grid export power at the minimum set level. $P_{Grid}^{Net}(max)$ is net grid import power at the maximum set level.

The components and system data are displayed in Table 3. Peak demand charge is considered occurring a peak load in during the on-peak time period. The objective of metaheuristic optimization methods is to identify viable solutions for intricate optimization challenges when conventional approaches are inadequate or inefficient. The OBC study evaluates the effectiveness of OBC-PSO and OBC-GA in optimizing BESS scheduling for energy management.

The OBC-PSO algorithm is widely recognized for its rapid convergence characteristics, procedural simplicity, and robust ability to locate global optima across high-dimensional search spaces (Zakeri *et al*., 2015; Khan *et al*., 2020; Jain *et al.,* 2020; Rasoulzadeh-akhijahani *et al*., 2015; Wu *et al.,* 2021). In this implementation, the iterative search process is driven by updating the velocity and position of each particle according to the stochastic governing equations (8) and (9), respectively (Khan *et al.,* 2020):

$$X_k(i+1) = X_k(i) + V_k(i+1) \quad (8)$$

$$V_k(i+1) = \omega V_k(i) + c_1 r_1 \left(p_{best,i}^k - X_k(i)\right) + c_2 r_2 \left(g_{best}, i - X_k(i)\right) \quad (9)$$

where i is the particle number. $X_k(i+1)$ is the position of a particle, i at the $(i+1)^{th}$ iteration. $V_k(i+1)$ is the vector of particle i at the $(i+1)^{th}$ iteration. ω is the inertia weight of a particle. c_1 and c_2 are the acceleration coefficient of the particle and the group, respectively. r_1 and r_2 are the uniformly distributed random numbers of the particle and the group, respectively, in the range from 0 to 1.

Table 3
The data of the components and system.

Parameters	Symbols	Values
Battery power and capacity	$\boldsymbol{P_B/E_B}$	100kW/227.2 kWh
Battery C-rate	*C-rate*	0.3
Initial SoC of the BESS	$\boldsymbol{SoC_{Start}}$	50%
Battery efficiency	$\boldsymbol{\eta_{BAT}}$	98%
SoC range	$\boldsymbol{SoC}$	20-80%
PCS charging efficiency	$\boldsymbol{\eta_{CHG}}$	80%
PCS discharging efficiency	$\boldsymbol{\eta_{DIS}}$	90%
Set discharging and charging battery power	$\boldsymbol{P_B^{min}}$, $\boldsymbol{P_B^{max}}$	-70 kW, +70 kW
Range of net grid export at minimum level and import power at maximum level	$\boldsymbol{P_{Grid}^{Net}(min)}$, $\boldsymbol{P_{Grid}^{Net}(max)}$	-120kW, +120 kW

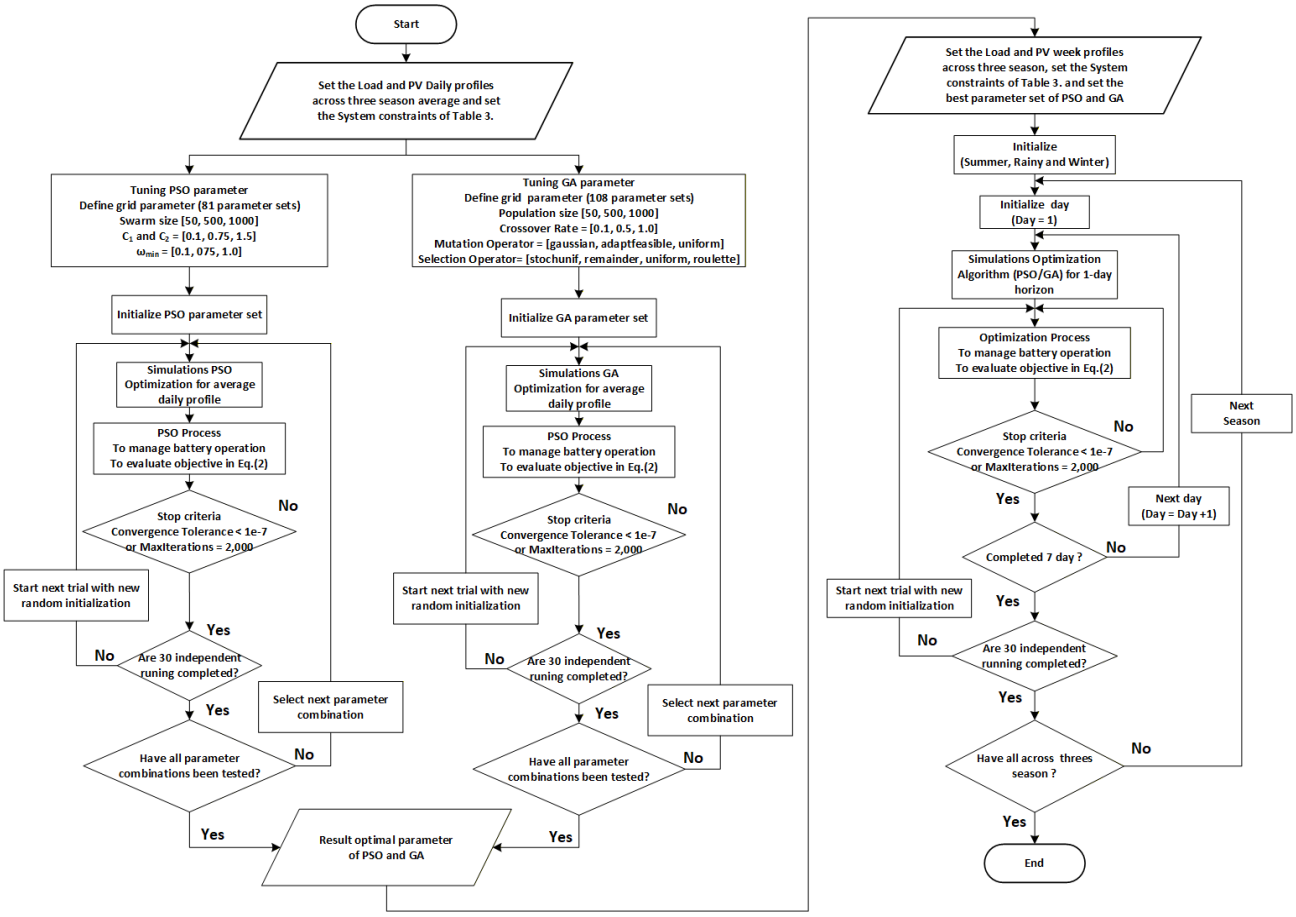


Fig 6. A framework for parameter tuning and sequential performance evaluation of OBC-PSO and OBC-GA.

An initiative framework for simultaneous tuning of parameters was implemented for both OBC-PSO and OBC-GA to ensure reproducible and statistically reliable selection of hyperparameters, as shown in Figure 6. The tuning procedure was carried out within a standard 1-day timeframe to achieve notable computational efficiency, leveraging load and PV profiles that were averaged over three seasons. The OBC-PSO was evaluated across 81 parameter sets: swarm size, c_1, c_2, and ω_{min} . Meanwhile the OBC-GA was assessed across 108 parameter settings: population size, crossover fraction, mutation, and selection operators. To ensure statistical significance, each parameter set was evaluated through 30 independent simulations, totaling 2,430 for OBC-PSO and 3,240 for OBC-GA. The optimal tuning parameter set for each algorithm was ultimately selected based on the condition with the lowest average objective value and a low standard deviation across the 30 independent simulations. The optimized tuning parameters were used subsequently in the pattern determination of battery charging-discharging.

Each algorithm, after optimizing its tuning parameters, was tested by considering average PV and load profiles over a week and in three seasons. The tests were set, with the SoC being carried over from the end of each day as the starting point for the next day. Furthermore, identical termination criteria were applied to both algorithms: a convergence tolerance of 10^{-7} or a maximum of 2,000 iterations, along with an additional stall limit of 50 iterations without improvement.

2.4 Economic and battery degaration analysis

The basic crucial financial metrics: discount payback time (DPB), net present value (NPV), internal rate of return (IRR), levelized cost of energy (LCOE), the equivalent annual cost (EAC) and the Net Present Cost (NPC) are necessary for comprehensive assessment of advanced PV systems (Karim *et al.*, 2025). Evaluating the economic benefits of the PV system with these metrics, they can serve as reliable criteria for future investment decisions.

The NPV is a financial metric that considers the discounted present value of projected future cash flows using an appropriate minimum required rate of return, as shown in the Equation (10). NPV positivity indicates financial feasibility, with negativity indicating an unprofitable venture.

$$\boldsymbol{NPV} = -\boldsymbol{C_0} + \sum_{\boldsymbol{n=1}}^{\boldsymbol{LT}} \frac{\boldsymbol{CF_n}}{\boldsymbol{(1+r)^n}} + \frac{\boldsymbol{S_{V,LT}}}{\boldsymbol{(1+r)^{LT}}} \quad (10)$$

where C_0 is the initial investment from the PV and BESS. CF_n represents the net cash flow in year n. The annual cash flow is derived from the revenue minus the regular operation and maintenance (O&M) costs. In specific years when the battery capacity degrades to its end-of-life threshold, the replacement cost is additionally deducted from the cash flow. On the other hand, at the end of the project year, the proportioned salvage value of the remaining battery life is refunded and added to the net cash flow as residual income. Furthermore, r is the discount rate, which is set at 7%, and LT indicates the total project lifetime of 25 years.

The salvage value ($S_{V,LT}$) represents the residual financial value of a component at the end of its lifespan. According to Equation (11), this value, which is designated as revenue, can be calculated.

Table 4
Economic analysis using the cost parameters of PV system (Ghadim *et al.,* 2025; Elmotech 2023).

Items	Details		
	Capital Cost for Initial Investment	Replacement Cost	Operation and Maintenance cost
PV +BOS	500 USD/kW$_p$	N/A	9.3 USD/kW$_p$
BESS	180 USD/kWh	180 USD/kWh	5.4 USD/kWh

Component cost (USD)	PV+BOS	BESS	Total costs
	69,120	40,896	110,016
% Fraction	62.82	37.18	100%

$$S_{V,LT} = C_R \frac{R_{rem}}{R_{comp}} \quad (11)$$

where R_{rem} is the remaining life of the component in years. R_{comp} is the lifetime of the component in years.

NPC, commonly known as the life cycle cost of the system, plays a pivotal role as a significant economic indicator, comparable to NPV. This valuation includes all capital and recurring expenditures over the 25-year operational duration of the system. This comprehensive assessment in the study incorporates initial capital investments, O&M costs, battery replacement costs, and the residual value of components over the entire life cycle. These costs can be calculated using Equation (12).

$$NPC = C_0 + \sum_{n=1}^{LT} \frac{C_{R,n}}{(1+r)^n} + \sum_{n=1}^{LT} \frac{C_{O\&M,n}}{(1+r)^n} - \frac{S_{V,LT}}{(1+r)^{LT}} \quad (12)$$

where $C_{R,n}$ is the cost of component replacement in year n. $C_{O\&M,n}$ is the operation and maintenance costs in year n.

The IRR represents the anticipated rate of return on an investment. The discount rate at which the NPV of a project becomes zero is shown in Equation (13) (Pinto *et al.,* 2024).

$$0 = -C_0 + \sum_{n=1}^{LT} \frac{CF_n}{(1+IRR)^n} \quad (13)$$

The EAC quantifies the annualized lifecycle expenditure of the system, facilitating a direct comparison between diverse investment scenarios by normalizing total costs over the operational horizon of the project. The EAC is derived from Equation (14) as follows:"

$$EAC = NPC \frac{(1+r)^{LT} r}{(1+r)^{LT}-1} \quad (14)$$

The LCOE represents the average expense of electricity generated per kilowatt-hour throughout the entire duration of the project. It is an important metric for evaluating the cost-effectiveness of different energy production technologies. LCOE can be calculated from the Equation (15).

$$LCOE = \frac{C_0 + \sum_{n=1}^{LT} \left[\frac{C_{O\&M,n} + C_{R,n}}{(1+r)^n}\right] - \frac{S_{V,LT}}{(1+r)^{LT}}}{\sum_{n=1}^{LT} \frac{E_{T,n}}{(1+r)^n}} \quad (15)$$

where E_T is the cumulative energy production each year n.

The DPB is primarily utilized to determine the years needed to achieve the break-even point and to assess financial risk and the duration of recovery for the initial investment. To determine the DPB, the annual CF_n must be converted into the discounted cash flow (DCF) to account for the time value of money, such an indicator is represented form by Equations (16) and (17).

$$DCF = \frac{CF_n}{(1+r)^n} \quad (16)$$

$$DPB = L + \frac{C}{A} \quad (17)$$

where L denotes the end of the year with the negative discounted cumulative cash flow. C is the absolute value of discounted cumulative cash flow at the end of the year L. A is the discounted cash flow during the period after L.

The total costs of the PV system components, including PV modules, the balance of system (BOS), BESS, installation, and O&M, are the subject of this study. Table 4 presents the installation, operation and maintenance costs of the system. The PV modules rely on the premise that the operational lifetime of the equipment fully encompasses the full 25-year project timeframe, as assured by the manufacturer. In this project of installed BESS capacity at 227.2kWh, its cost is about 35% of the total costs of the PV system.

In this work, the battery life loss is related to its degradation and charging-discharging trajectories derived from each EMS strategy. To calculate the total health effect, the weekly SoC profiles are analyzed with the rainflow-counting algorithm, as implemented in MATLAB. This algorithmic methods facilitates the identification of both half and full cycles across varying DOD levels, which is critical for capturing the non-linear nature of battery aging in prosumer system applications.

Battery self-degradation is linked to internal material deterioration, which is set to 15 years, meaning it degrades at 6.67% per year. The cumulative battery life loss ($Life_{loss}$) is calculated by aggregating the losses from individual cycles according to Equation (18):

$$\boldsymbol{Life_{loss} = \sum_{j=1} \frac{N_{cycle,j}}{\eta_{100}} \times d_{cycle,j}^{DegB} \quad \text{for } j = 1, 2, 3, \ldots} \quad (18)$$

where $Life_{loss}$ is the loss of battery life during half/full cycles compared with the beginning of the battery life. $N_{cycle,j}$ is the number of cycles. j denotes the index of the identified cycle, d_{cycle} is the cycle depth, equivalent to the DOD for each identified event. η_{100} is the total number of battery cycles of 4000 cycles (at 100% DOD). $DegB$ is the curve's slope of the degradation setting at 1.0 for the 0.3 C-rate.

4. Simulation Results and Discussion

To evaluate the impact of seasonal weather variability on optimal BESS scheduling, PV power generation uncertainty was analyzed across three distinct periods: summer (three months), rainy season (five months), and winter (four months). The daily

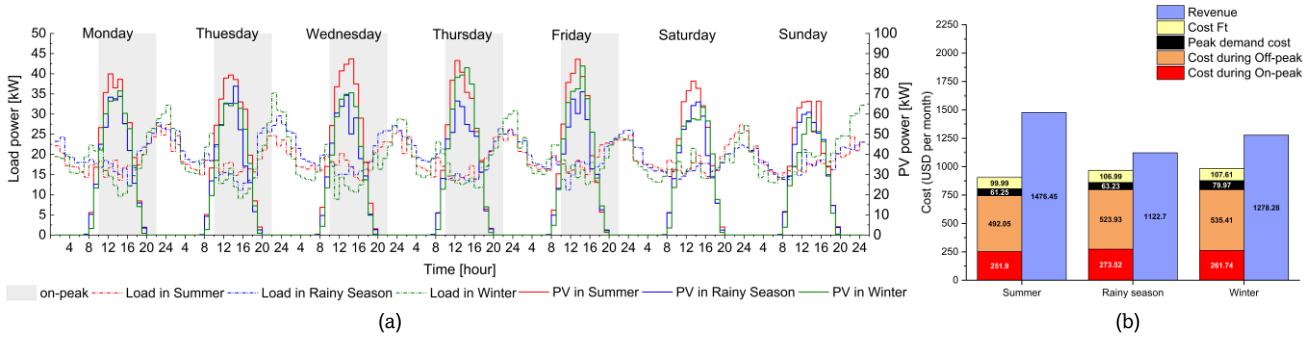


Fig 7. (a) Seasonal load profiles and (b) Revenue and electricity costs during on/off peaks

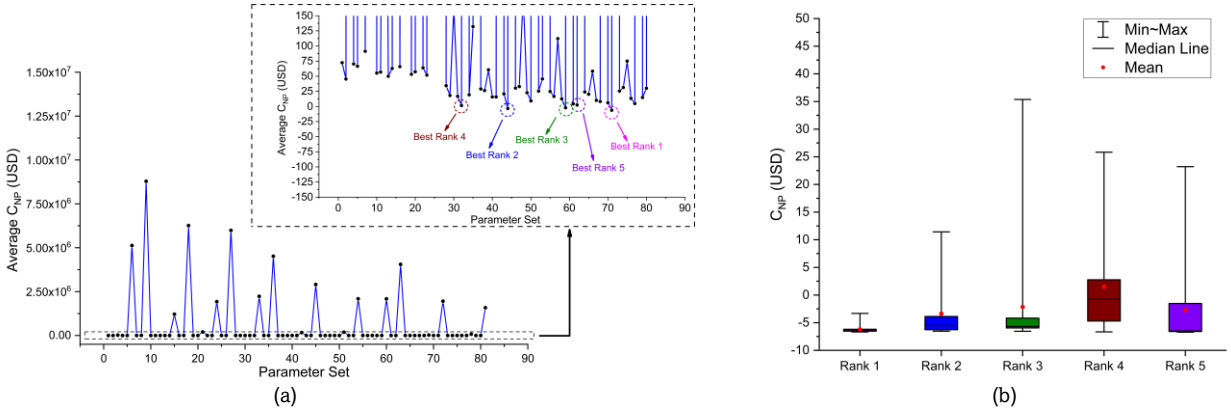


Fig 8. OBC-PSO hyperparameter tuning results: (a) distribution of mean objective values across 81 evaluated parameter configurations, and (b) statistical variation and robustness analysis of the top five ranked parameter sets over 30 independent simulations.

average PV generation and load demand data (assuming no BESS) are presented as weekly profiles in Figure 7(a). The energy demands of the S5 prosumer are lower than those of the installed PV system. It appears that summer PV generation is higher weekly compared to other seasons, while peak-load powers in the evening exhibit higher values predominantly in winter (35.28kW). The energy demand values in the three seasons exhibit quite similar levels (3.15 MWh-3.21 MWh), with only a 2.34% difference. The profiles are discussed in terms of electricity costs during on/off peak times and revenues from energy sales as illustrated in Figure 7 (b). Across all seasons, lower electricity costs during on-peak times are shown because the demand during on-peak times is met by generated PV power, reducing the demand for additional electricity. Meanwhile, the peak energy harvested from PV is observed in summer because of the maximal PV energy production.

Utilizing the representative seasonal profiles, the hyperparameter tuning process for both OBC-PSO and OBC-GA was conducted to identify the optimal configuration for BESS scheduling. The resulting fitness values are illustrated in Figures 8(a)-(b) and 9(a)-(b) for the OBC-PSO and OBC-GA metaheuristics, respectively. In this study, the objective function is formulated as a minimization problem, where increasingly negative values represent maximized prosumer net profit. For the OBC-PSO, a systematic grid search across 81 configurations was performed, yielding a superior average objective C_{NP} score

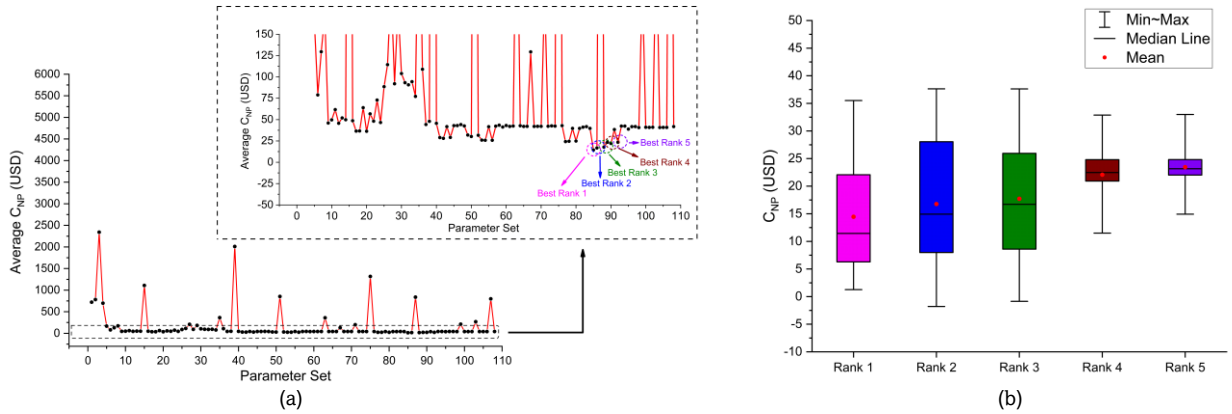


Fig 9. OBC-GA hyperparameter tuning results: (a) distribution of mean objective values across 81 evaluated parameter configurations, and (b) statistical variation and robustness analysis of the top five ranked parameter sets over 30 independent simulations.

Table 5
Results of the optimal parameter sets calculated from simultaneous OBC-PSO and OBC-GA tuning processes.

OBC Algorithm	Parameter sets	Average of C_{NP} (USD)	S.D.
PSO (Rank 1)	Swarm size = 1,000, C_1 = 0.75, C_2 = 1.5, ω_{min} = 0.75	-6.19	0.67
PSO (Rank 2)	Swarm size = 500, C_1 = 0.75, C_2 = 1.5, ω_{min} = 0.75	-3.36	4.86
PSO (Rank 3)	Swarm size = 1000, C_1 = 0.1, C_2 = 0.75, ω_{min} = 0.75	-2.14	9.40
PSO (Rank 4)	Swarm size = 500, C_1 = 1.5, C_2 = 0.75, ω_{min} = 0.75	1.50	8.56
PSO (Rank 5)	Swarm size = 1,000, C_1 = 0.1, C_2 = 1.5, ω_{min} = 0.75	2.46	31.48
GA (Rank 1)	Population size = 1,000, Crossover Rate = 0.5, Mutation Operator = gaussian, Selection Operator = stochunif	14.45	10.38
GA (Rank 2)	Population size = 1,000, Crossover Rate = 0.5, Mutation Operator = gaussian, Selection Operator = remainder	16.76	11.61
GA (Rank 3)	Population size = 1,000, Crossover Rate = 0.5, Mutation Operator = gaussian, Selection Operator = roulette	17.72	10.84
GA (Rank 4)	Population size = 500, Crossover Rate = 0.5, Mutation Operator = adaptfeasible Selection Operator = remainder,	22.08	4.16
GA (Rank 5)	Population size = 500, Crossover Rate = 0.5, Mutation Operator = adaptfeasible, Selection Operator = roulette	23.44	3.37

Note: Positive and negative values of C_{NP} represent the cost of a higher purchase than selling and a higher selling than purchase, respectively.

of -6.19 USD (the cost of a higher selling than purchase). As shown in the statistical distribution (Figure 8b), the highest-ranked configuration (Rank 1) demonstrated high stability, with a standard deviation (S.D.) of only 0.67. Notably, an inertia weight (ω_{min}) of 0.75 was consistent across all top-ranked OBC-PSO configurations, suggesting that a moderate inertia weight is vital for balancing global exploration and local exploitation under TOU tariff constraints.

In contrast, the OBC-GA provided the best average objective values remaining positive (ranging from 14.45 to 23.44 USD). This disparity indicates a failure to attain the same levels of profitability as the OBC-PSO strategy. Furthermore, the OBC-GA exhibited substantial instability, evidenced by a high S.D. of 10.38 in its top-ranked parameter set. This high variance suggests that the OBC-GA is more susceptible to trapping in local optima when applied to this specific scheduling problem. The statistical performance of the top five configurations for each algorithm is summarized in Table 5, serving as the basis for the final BESS scheduling optimization.

The operational efficacy of the BESS scheduling strategies was evaluated by analysing the convergence behaviour of the metaheuristic algorithms across varying seasonal conditions. Figures 10(a)-(c) illustrate these dynamics through a representative daily profile, highlighting a distinct trade-off between convergence pattern and solution optimality. The OBC-GA framework demonstrated superior computational efficiency, achieving shorter processing time than the OBC-PSO counterpart. However, this accelerated performance was offset by a propensity for premature convergence, where the OBC-GA proved susceptible to being trapped in local optima, a common limitation in complex, non-linear search spaces.

In contrast, The OBC-PSO algorithm exhibited superior global search capabilities, effectively navigating the solution space to escape local optima. This resulted in a significantly more refined objective value, surpassing the OBC-GA outcomes by 2.60% to 8.76%. While the OBC-PSO requires a higher computational investment, the subsequent enhancement in solution quality provides a more robust foundation for long-term revenue optimization. Consequently, the findings suggest that for prosumer-scale energy management, the OBC-PSO approach provides a meaningful improvement in financial optimality.

The resulting seasonal charge-discharge patterns and SoC profiles are depicted in Figures 11(a)-(c). To provide a rigorous comparative assessment of the electrochemical stress imposed by each strategy, the cycle depth (d_{cycle}) and cumulative cycle counts (N_{cycle}) were evaluated. A primary finding is that the RBC mechanism consistently yields higher N_{cycle} values, a direct

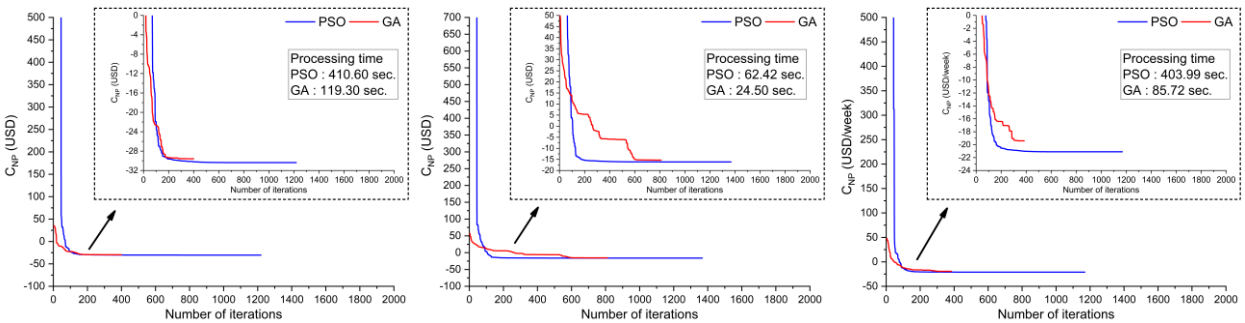


Fig 10. The comparison of algorithm convergence for OBC-PSO and OBC-GA during a day of each season in this example shown on Monday with results presented for (a) Summer, (b) Rainy season, and (c) Winter.

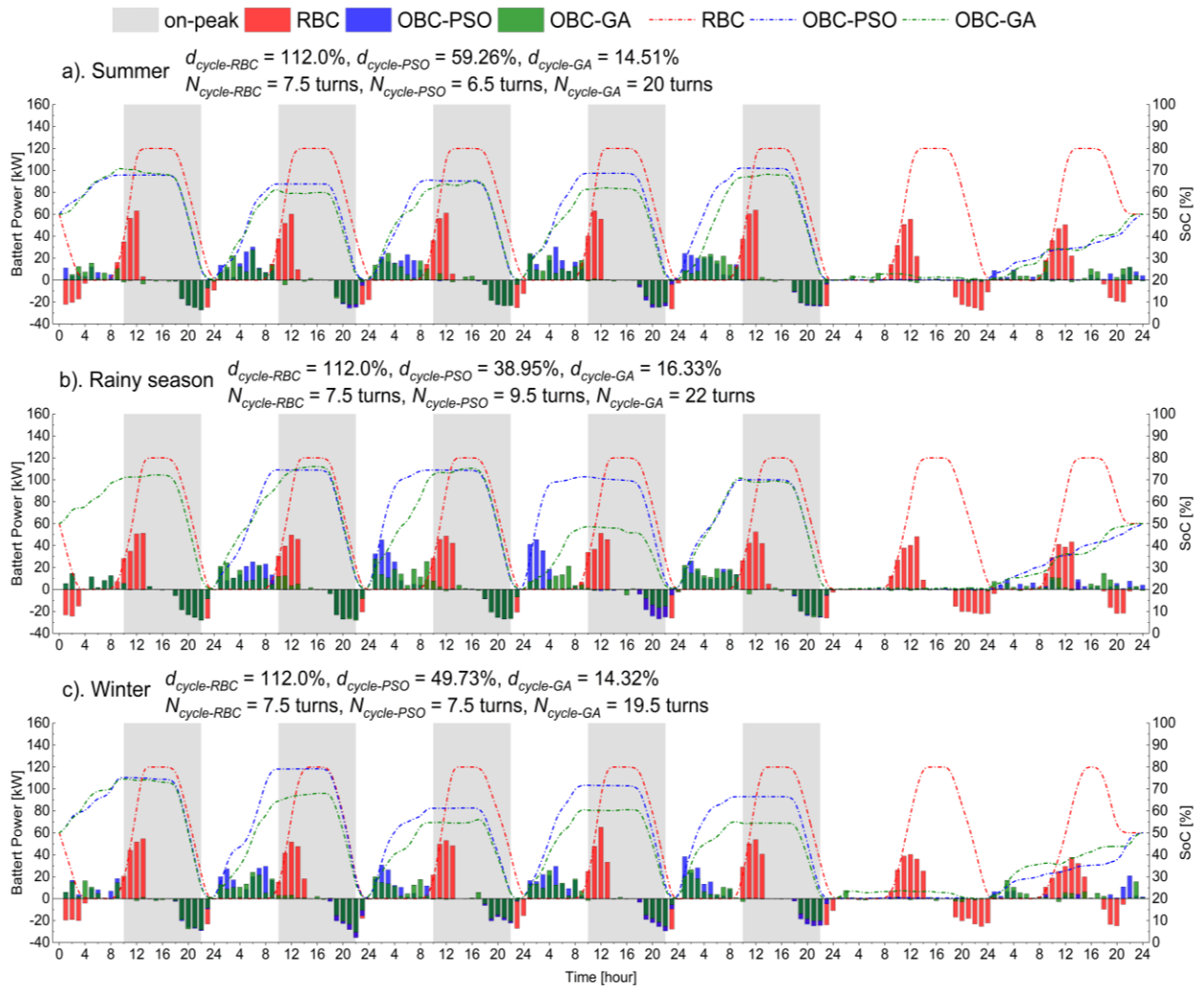


Fig 11. Comparison of charging and discharging patterns and SoC of the battery under using the RBC, OBC-PSO, and OBC-GA in (a) summer, (b) rainy season, and (c) winter.

consequence of its deterministic heuristic aimed at maintaining instantaneous grid neutrality ($P_{Grid}^{NET}(t) = 0$). This rigid operational logic forces the system into frequent, shallow charging phases during peak PV generation, followed by complete discharge cycles at night. Such scheduling patterns are particularly pronounced during the summer months, where the RBC strategy exhibits constrained charging windows and elevated d_{cycle} values compared to the rainy and winter seasons.

Contrary to the heuristic approach, both OBC strategies strategically capitalize on TOU price variations to maximize energy arbitrage. This is achieved by shifting charging periods to low-cost off-peak hours and discharging during high-cost on-peak intervals. Notably, the percentage of d_{cycle} per a cycle for the OBC-PSO (38.95%-59.26%) was significantly higher than that of the OBC-GA (14.32%-16.33%). The N_{cycle} for the OBC-PSO (9.5-6.5 turns) was significantly higher than that of the OBC-GA (19.5-22.0 turns). This elevation in d_{cycle} correlates with a lower N_{cycle} suggesting that both d_{cycle} and N_{cycle} reflect the percentage of battery life loss. Furthermore, winter profiles exhibit extended discharge durations to meet higher load demands. These dynamic, non-uniform operational characteristics align with recent findings in Home Energy Management Systems (HEMS) and smart microgrid literature (Korab *et al.,* 2026; Masoumi-Anaraki *et al.*, 2025).

A comparative analysis of seasonal power profiles (Appendix: Figures A1-A3) shows that OBC strategies result in higher energy exchange (imports and exports) than RBC, reflecting a more aggressive utilization of the storage capacity to meet economic objectives. While both RBC and OBC-PSO successfully perform comprehensive peak shaving across all seasons, the OBC-GA strategy fails to eliminate peaks entirely, leaving residual demands of 2.8-9.8 kW as shown in Appendix: Figures A1(c)-A3(c). This performance gap is primarily attributed to the superior convergence capabilities of the OBC-PSO algorithm, which is more effective at identifying globally optimal schedules. Such effective peak demand mitigation is critical for minimizing demand charges and reducing overall prosumer electricity expenditures.

The seasonal and annual performance metrics for the PV-BESS prosumer are summarized in Table 6. The data indicate that the RBC strategy fails to exploit TOU energy arbitrage, instead relying on heuristic if-then rules to maximize self-consumption based on established expert knowledge (Zhou *et al.,* 2023) Conversely, the OBC strategies utilize dynamic decision-making to optimize BESS scheduling, resulting in significant off-peak imports and maximized energy exports. This behavior aligns with contemporary research regarding the profitability of optimized storage systems (Mquqwana *et al.,* 2024; Wang *et al.,* 2021; Kumar *et al.,* 2024; Recalde *et al.,* 2024).

Yearly evaluations demonstrate that both OBC strategies maintain a significant profitability advantage over RBC. OBC-PSO yields the highest annual net profit at 23,544 USD, a 13.5% increase over RBC (20,742 USD), followed by OBC-GA at 23,174 USD. The economic benefit is particularly evident in summer,

Table 6
The data summary of average values of energy imports and exports, net profit and battery life loss of S5 prosumer from utilizing RBC, OBC-PSO, and OBC-GA strategies.

Season	Strategy	Average PV Generation (kWh/month)	Average Energy Import (kWh/month)	Average Energy Export (kWh/month)	Average Net Profit (USD /month)	Average Life Loss of Battery (%/month)
Summer (total 3 months)	RBC	17,126.08	4,421.41	6,564.38	1,984	0.46
	OBC-PSO		8,829.08	11,713.01	2,216	0.26
	OBC-GA		8,631.31	11,449.41	2,196	0.26
Rainy (total 5 months)	RBC	14,065.21	4,995.28	3,758.52	1,594	0.46
	OBC-PSO		9,492.21	8,901.13	1,824	0.29
	OBC-GA		9,233.60	8,637.31	1,782	0.27
Winter (total 4 months)	RBC	14,662.39	5,043.91	4,790.64	1,705	0.46
	OBC-PSO		9,649.22	10,073.39	1,944	0.28
	OBC-GA		9,450.88	9,917.89	1,919	0.24
Season	Strategy	Average PV Generation (kWh/year)	Average Energy Import (kWh/year)	Average Energy Export (kWh/year)	Average Net Profit (USD /year)	Average Life Loss of Battery (%/year)
Year round	RBC	180,353.90	58,416.24	57,594.78	20,742	5.47
	OBC-PSO		112,545.20	119,938.22	23,544	3.30
	OBC-GA		109,865.10	117,206.31	23,174	3.11

when an average of 17,126.08 kWh is produced each month. This allows the OBC-PSO to maximize on-peak sales, leading to an especially high monthly profit of 2,216 USD. Annual energy exports under the OBC-PSO strategy rose by 108% relative to the RBC baseline, increasing from 57,594 to 119,938 kWh/year. This significant growth signifies the efficacy of the active TOU arbitrage mechanism, wherein the optimization algorithm leverages the BESS to store energy during off-peak intervals and maximize revenue through targeted on-peak exports.

A notable finding is the relationship between OBC-induced trading activity and battery degradation. Although OBC strategies engage in significantly higher energy trading than RBC, the annual battery life loss under OBC-PSO (3.30%) and OBC-GA (3.11%) is reduced by 39.7% and 43.1%, respectively, compared to RBC (5.47%). This is primarily attributed to the deeper average cycles (d_{cycle}) facilitated by the OBC-PSO algorithm to capture arbitrage opportunities. While RBC induces uncoordinated and inefficient cycling, the optimization strategies concentrate battery operation during on-peak times, resulting in more economically productive cycles that preserve battery state of health. Thus, the OBC-PSO strategy results in approximately 2,802 USD annually, alongside reducing battery degradation. This indicates that optimization provides the efficient BESS scheduling for the RES (Wang *et al.,* 2024).

The system showcases a notable responsiveness to Thailand's seasonal climate. During the rainy season, when the monthly PV generation is at its lowest (14,065.21kWh), OBC-PSO maintains financial resilience with a monthly net profit of 1,824 USD. Simultaneously, it provides a 14.42% improvement over RBC confirming that the algorithm adapts effectively to reduced irradiance conditions by shifting reliance toward grid arbitrage rather than PV export. During winter, OBC-GA achieves the lowest monthly battery life loss of 0.24%, reflecting a more conservative dispatch pattern suited to lower solar surplus. Overall, OBC-PSO demonstrates the most consistent seasonal performance, maintaining monthly net profit within a narrow range of 1,824-2,216 USD across all seasons with the smallest seasonal variance among the three strategies.

Based on a longitudinal assessment of DoD and self-degradation, the BESS under the RBC strategy reaches its End-of-Life (EoL) threshold within eight years. In contrast, the OBC frameworks extend this operational lifespan to ten years, achieving a 25% improvement in lifecycle durability. These findings demonstrate that the proposed optimization strategies successfully harmonize aggressive revenue maximization with hardware sustainability, thereby significantly mitigating the frequency of capital-intensive reinvestment. Such outcomes confirm that these optimization frameworks effectively resolve the inherent trade-off between energy arbitrage intensity and electrochemical health preservation, as consistent with the research of Lee and Kim (2022).

The 25-year longitudinal economic indices for the evaluated prosumer system are summarized in Table 7, integrating BESS lifecycle replacement costs derived from degradation modeling. The application of meta-heuristic optimization (OBC-PSO and OBC-GA) demonstrates a transformative impact on project bankability compared to the conventional RBC baseline. Specifically, the OBC-PSO strategy achieved the highest financial performance, yielding an IRR of 8.98% and an NPV of 97,639 USD, nearly doubling the net value relative to the RBC approach (IRR: 4.34%; NPV: 49,171 USD). Crucially, the optimization frameworks significantly accelerate capital recovery, contracting the DPB from 11.71 years (RBC) to just 6.74 years (OBC-PSO). This substantial 4.97-year reduction in DPB effectively de-risks the investment, providing a more resilient financial roadmap over the multi-decade operational horizon.

Regarding cost efficiency, both OBC strategies achieved an identical reduction in the LCOE to 0.078 USD/kWh, representing an 8.23% improvement over the RBC baseline (0.085 USD/kWh). This optimization further resulted in a substantial decrease in the NPC, from 195,060 USD to 179,362 USD, and the EAC, from 16,738 USD to 15,391 USD per year. These values are highly consistent with the benchmarks established by Do et al. (2025), who reported a PV-BESS LCOE

Table 7
Economic outcomes with non-considering BESS discount and considering BESS replacement of S5 prosumer from utilizing RBC, OBC-PSO, and OBC-GA strategies.

Detail	Strategies		
	RBC	OBC-PSO	OBC-GA
IRR (%)	4.34	8.98	8.60
DPB (years)	11.71	6.74	6.90
LCOE (USD/kWh)	0.085	0.078	0.078
NPV (USD)	49,171	97,639	93,211
NPC (USD)	195,060	179,362	179,362
EAC (USD)	16,738	15,391	15,391

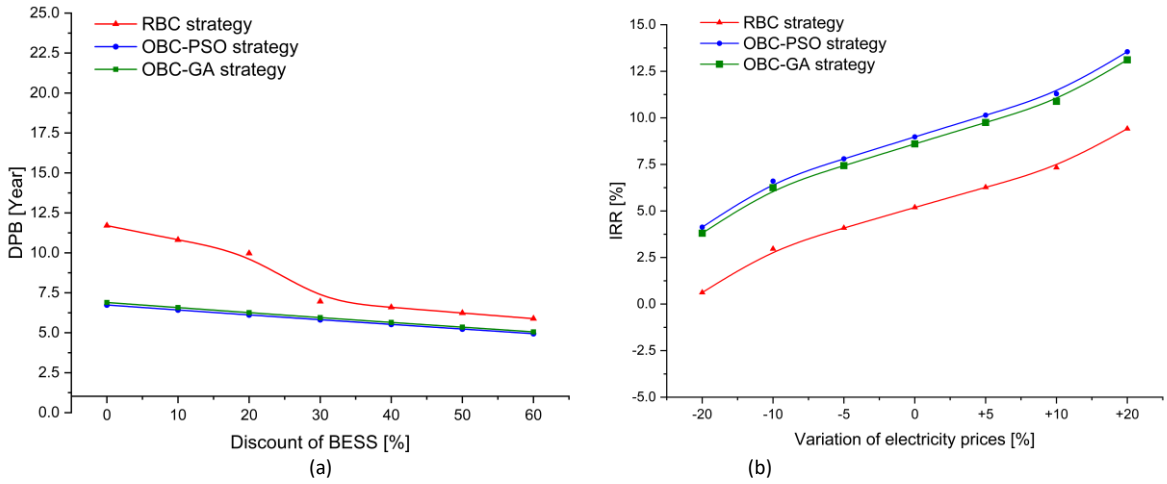


Fig 12. Sensitivity analysis of financial performance: (a) discounted payback period under varying BESS capital cost reductions, and (b) IRR under electricity tariff variations (-20% to +20%) for RBC, OBC-PSO, and OBC-GA strategies.

range of 0.0638-0.0937 USD/kWh. Notably, even including the BESS replacement costs, maintaining the 0.078 USD/kWh figure of this prosumer project continues to be economically competitive.

Although both metaheuristic algorithms converge on the same cost minimum, the OBC-PSO strategy demonstrated superior revenue-generation capabilities, yielding a 4,428 USD higher NPV than the OBC-GA. This financial edge is primarily attributed to the more effective scheduling of peak-period exports by the OBC-PSO strategy. Collectively, the achievement of an 8.98% IRR and the compression of the payback period to under seven years transitions the prosumer system into a highly bankable asset. These findings confirm that project feasibility is increasingly dictated by control architecture design rather than hardware capacity alone.

Furthermore, the reduced LCOE narrows the margin toward grid parity and provides a critical financial buffer against market uncertainties. These outcomes indicate that OBC strategies, underpinned by systematic parameter tuning, deliver significantly more favorable economic results than the RBC benchmark. This performance is driven by a dual-benefit mechanism: the mitigation of battery degradation expenditures and the simultaneous enhancement of trading revenues through optimized dispatch. These insights align with the findings of Rana and Gróf (2024), who demonstrated that prosumer-centric trading and optimal scheduling are essential for substantial reductions in total system costs and LCOE in decentralized energy markets.

As depicted in Figure 12(a), when evaluating projected BESS capital cost reductions (ranging from 0% to 60%), the two proposed OBC strategies exhibit a more stable DPB compared to the rule-based control (RBC) strategy. Both OBC approaches demonstrate a linear decrease in DPB as BESS costs decline, with merely a marginal 2% variance between them. Notably, below a 30% cost reduction range, the OBC strategies achieve a significantly lower DPB than the RBC baseline. This performance gap is primarily attributed to the higher frequency of BESS replacements required under the RBC strategy (three replacements), which severely diminishes its discounted cumulative cash flows.

Furthermore, as BESS cost reductions exceed 30%, the RBC strategy effects result in a significant decrease in DPB in its cumulative cash flow. In contrast, the OBC-PSO algorithm maintains a consistent and linear reduction in DPB, ultimately achieving an accelerated investment recovery of 4.95 years at a 60% cost reduction. This trend aligns with the sensitivity analysis conducted by Purohit et al., 2026, which corroborates that declining storage capital expenditures directly accelerate capital recovery timelines, reducing payback periods to 4-5 years, thereby enhancing overall project feasibility.

Beyond the capital cost sensitivities shown in Figure 12(b), the proposed OBC framework exhibits strong financial flexibility in response to electricity tariff variations between -20% and 20%. Under these conditions, both OBC strategies effectively manage the IRR, exhibiting a decrease of 4.8% during a 20% tariff drop, and a corresponding increase of 4.5% during a 20% tariff surge. By precisely scheduling BESS operations to leverage TOU arbitrage, the OBC framework fundamentally optimizes total cash flow, significantly enhancing the IRR and overall profitability of the PV-BESS project under upward tariff trends.

6. Conclusion

A comprehensive techno-economic evaluation of a grid-tied PV-BESS prosumer system is presented emphasizing the critical role of algorithm initialization and simultaneous parameter tuning in energy management. Developing a rigorous framework for optimizing the hyperparameters of PSO and GA demonstrates a significant advancement over conventional heuristic methods, such as the RBC method.

Both OBC strategies substantially outperform RBC in techno-economic performance. Exploiting dynamic decision-making to optimize BESS patterns results in large off-peak imports and maximum energy exports. Compared to RBC, OBC-PSO and OBC-GA increase the annual net profit by 13.50% and 11.72%, respectively. OBC-GA converges 60.74-78.78% faster than OBC-PSO but OBC-PSO outperforms in objective values by 2.60-8.76%, enhancing economic returns consistently.

The battery degradation analysis verifies that enhanced scheduling directly influences lifecycle costs. OBC strategies help in reducing the average annual battery life loss from 5.47% (RBC) to approximately 3.11-3.30%, thereby extending the effective replacement cycle from 8 (RBC) to 10 years, assuming a 30% capacity fade threshold. This two-year extension in the replacement interval is a major driver of long-term cost reduction. Over a 25-year horizon, OBC-PSO achieves an IRR of 8.98%, the NPV of 97,639 USD, and reduces the DPB from 11.71 years (RBC) to 6.74 years. LCOE, NPC, and EAC are also improved, with LCOE reduced from 0.085 to 0.078 USD/kWh and NPC from 195,060 to 179,362 USD.

The proposed tuning-centric OBC framework, as further confirmed by sensitivity and robustness analyses, provides a significant financial buffer against market volatility. Demonstrating robust financial performance, the system achieved a high IRR of approximately 13.54%. Even under challenging conditions, such as a 20% reduction in electricity tariffs, the OBC-PSO approach maintained economic viability with an IRR of 4.12%, whereas the RBC strategy became less economically advantageous

In summary, this research underscores that the commercial viability of grid-tied prosumer systems is driven not only by hardware costs but, more crucially, by the mathematical precision of the energy management framework. The systematic initialization and tuning process introduced here provide a scalable and reliable model for optimizing energy trading in university campuses and emerging smart communities, ensuring long-term sustainability in an evolving energy landscape.

Acknowledgments

This work was supported by Suranaree University of Technology (SUT) Research and Development Fund, Thailand.

Author Contributions: Hideki Kakhai: Methodology, formal analysis, writing original draft, Thipwan Fangsuwannarak: supervision resources, conceptualization, project administration, validation, writing review, editing, Jirut Rhianprayoon; project administration, validation, Reungpong Reunghirun; project administration, validation.

Funding: SUT Research and Development Fund

Conflicts of Interest: No conflict of interest.

References

Abdul Basit, N. A. I., Rosmin, N., Mustaamal, A. H., Hussin, S. M., & Said, D. M. (2022). A simple energy management system for a micro grid system using rule-based algorithm. In *Control, instrumentation and mechatronics: theory and practice* (pp. 273-284). Singapore: Springer Nature Singapore. https://doi.org/10.1007/978-981-19-3923-5_24

Adenuga OT, Krishnamurthy S. Economic Power Dispatch of a Grid-Tied Photovoltaic-Based Energy Management System: Co-Optimization Approach. *Mathematics*. 2023; 11(15):3266. https://doi.org/10.3390/math11153266

Behzadi, A., & Sadrizadeh, S. (2023). Grid-tied solar and biomass hybridization for multi-family houses in Sweden: An optimal rule-based control framework through machine learning approach. *Renewable energy*, *218*, 119230. https://doi.org/10.1016/j.renene.2023.119230

Çınar H, Kandemir I. Active Energy Management Based on Meta-Heuristic Algorithms of Fuel Cell/Battery/Supercapacitor Energy Storage System for Aircraft. *Aerospace*. 2021; 8(3):85. https://doi.org/10.3390/aerospace8030085

Cole, W., Frazier, A. W., & Augustine, C. (2021). *Cost projections for utility-scale battery storage: 2021 update* (No. NREL/TP-6A20-79236). National Renewable Energy Lab.(NREL), Golden, CO (United States). https://doi.org/10.2172/1786976

de Lima, T. D., Faria, P., & Vale, Z. (2026). Optimal scheduling of home energy systems considering battery aging and CO2 emissions. *Applied Energy*, *409*, 127433. https://doi.org/10.1016/j.apenergy.2026.127433

Do, L. T., Nguyen, T. N., Tran, Q. T., & Duong, K. T. (2025). Economic analysis of solar power plant and battery energy storage: Case study of Binh Phuoc province, Vietnam. *Cleaner Engineering and Technology*, 26, 100937. https://doi.org/10.1016/j.clet.2025.100937

Elmotech. (2023, January 17). Thai BESS introduction & Southeast Asia market entry strategy. https://www.elmotech.co.th/en/blog-posts/thai-bess-introduction-southeast-asia-market-entry-strategy

Fadil, H. E., Idrissi, Z. E., Intidam, A., Rachid, A., Koundi, M., & Bouanou, T. (2020). Nonlinear control and energy management of the hybrid fuel cell and battery power system. *International Journal of Modelling, Identification and Control*, *36*(2), 89-103. https://doi.org/10.1504/IJMIC.2020.116196

Gbadega, P. A., & Balogun, O. A. (2025). Transactive energy management for efficient scheduling and storage utilization in a grid-connected renewable energy-based microgrid. *e-Prime-Advances in Electrical Engineering, Electronics and Energy*, 11, 100914. https://doi.org/10.1016/j.prime.2025.100914

Ghadim, H. V., Haas, J., Breyer, C., Gils, H. C., Read, E. G., Xiao, M., & Peer, R. (2025). Are we too pessimistic? Cost projections for solar photovoltaics, wind power, and batteries are over-estimating actual costs globally. *Applied Energy*, *390*, 125856. https://doi.org/10.1016/j.apenergy.2025.125856

Hadjipaschalis, I., Poullikkas, A., & Efthimiou, V. (2009). Overview of current and future energy storage technologies for electric power applications. *Renewable and sustainable energy reviews*, *13*(6-7), 1513-1522. https://doi.org/10.1016/j.rser.2008.09.028

Hafeez, G., Ullah, S., Islam, M., Khan, F. A., Alsafran, A. S., Alghamdi, B., & Kraiem, H. (2025). An improved meta-heuristic algorithm for energy optimization in smart grids considering photovoltaic, storage battery, and demand response. *Journal of Energy Storage*, *119*, 115929. https://doi.org/10.1016/j.est.2025.115929

Hasan, S., Zeyad, M., Ahmed, S. M., & Anubhove, M. S. T. (2023). Optimization and planning of renewable energy sources based microgrid for a residential complex. *Environmental Progress & Sustainable Energy*, *42*(5), e14124. https://doi.org/10.1002/ep.14124

Jain, M., Saihjpal, V., Singh, N., & Singh, S. B. (2022). An Overview of Variants and Advancements of PSO Algorithm. *Applied Sciences*, *12*(17), 8392. https://doi.org/10.3390/app12178392

Karim, F., Ahmed, T., & Rasif, M. H. I. (2025). Techno-economic assessment of utility-scale solar PV systems in south-eastern Bangladesh: Insights from empirical data and simulation modeling. *Energy Conversion and Management: X*, 101374. https://doi.org/10.1016/j.ecmx.2025.101374

Khan, A., Bressel, M., Davigny, A., Abbes, D., & Ould Bouamama, B. (2025). Comprehensive Review of Hybrid Energy Systems: Challenges, Applications, and Optimization Strategies. *Energies*, *18*(10), 2612. https://doi.org/10.3390/en18102612

Khan, A., Hizam, H., bin Abdul Wahab, N. I., & Lutfi Othman, M. (2020). Optimal power flow using hybrid firefly and particle swarm optimization algorithm. *Plos one*, *15*(8), e0235668. https://doi.org/10.1371/journal.pone.0235668

Khan, S. U. D., Wazeer, I., Almutairi, Z., & Alanazi, M. (2022). Techno-economic analysis of solar photovoltaic powered electrical energy storage (EES) system. *Alexandria Engineering Journal*, *61*(9), 6739-6753. https://doi.org/10.1016/j.aej.2021.12.025

Korab, R., Połomski, M., Smołka, M., & Naczyński, T. (2026). Impact of distributed battery energy storage controlled by optimization-based home energy management systems implementing various objective functions on the voltage profiles in the low-voltage network with a high saturation of prosumer photovoltaic micro-installations. *Energy Conversion and Management*, *353*, 121148. https://doi.org/10.1016/j.enconman.2026.121148

Kumar, R. P., & Karthikeyan, G. (2024). A multi-objective optimization solution for distributed generation energy management in microgrids with hybrid energy sources and battery storage system. *Journal of Energy Storage*, *75*, 109702. https://doi.org/10.1016/j.est.2023.109702

Lee, J. O., & Kim, Y. S. (2022). Novel battery degradation cost formulation for optimal scheduling of battery energy storage systems. International Journal of Electrical Power & Energy Systems, 137, 107795. https://doi.org/10.1016/j.ijepes.2021.107795

Luo, L., Abdulkareem, S. S., Rezvani, A., Miveh, M. R., Samad, S., Aljojo, N., & Pazhoohesh, M. (2020). Optimal scheduling of a renewable based microgrid considering photovoltaic system and battery energy storage under uncertainty. *Journal of Energy Storage*, *28*, 101306. https://doi.org/10.1016/j.est.2020.101306

Masoumi-Anaraki, M., Hooshmand, R. A., & Kabiri-Renani, Y. (2025). Probabilistic Pricing for Collaborative Demand-Side Management With Coordinated Operation of Energy Storage Systems for Optimal Peak Load Control in Smart Grids. *IET Generation, Transmission & Distribution*, *19*(1), e70084. https://doi.org/10.1049/gtd2.70084

Mohamed, A. A. R., Best, R. J., Liu, X., & Morrow, D. J. (2021). A comprehensive robust techno-economic analysis and sizing tool for the small-scale PV and BESS. *IEEE transactions on energy conversion*, *37*(1), 560-572. https://doi.org/10.1109/TEC.2021.3107103

Mouna, E. Q., Abbou, A., Laamim, M., Id-Khajine, L., & Rochd, A. (2025). Comparative analysis of GA and PSO algorithms for optimal cost management in on-grid microgrid energy systems with PV-battery integration. *Global Energy Interconnection*. https://doi.org/10.1016/j.gloei.2025.05.003

Mquqwana MA, Krishnamurthy S. Particle Swarm Optimization for an Optimal Hybrid Renewable Energy Microgrid System under Uncertainty. *Energies*. 2024; 17(2):422. https://doi.org/10.3390/en17020422

Njoka, G. M., Mogaka, L., & Wangai, A. (2025). Enhancing grid stability and resilience through BESS optimal placement and sizing in VRES-dominated systems. *Energy Reports*, *13*, 1764-1779. https://doi.org/10.1016/j.egyr.2025.01.028

Palizban, O., & Kauhaniemi, K. (2016). Energy storage systems in modern grids—Matrix of technologies and applications. *Journal of Energy Storage*, *6*, 248-259. https://doi.org/10.1016/j.est.2016.02.001

Pan, X., Khezri, R., Mahmoudi, A., Yazdani, A., & Shafiullah, G. (2021). Energy Management Systems for Grid-Connected Houses with Solar PV and Battery by Considering Flat and Time-of-Use Electricity Rates. *Energies*, *14*(16), 5028. https://doi.org/10.3390/en14165028

Patrizi, N., LaTouf, S. K., Tsiropoulou, E. E., & Papavassiliou, S. (2022). Prosumer-centric self-sustained smart grid systems. *IEEE Systems Journal*, *16*(4), 6042-6053. https://doi.org/10.1109/JSYST.2022.3156877

Pinto, G. X. A., Naspolini, H. F., & Rüther, R. (2024). Assessing the economic viability of BESS in distributed PV generation on public buildings in Brazil: A 2030 outlook. *Renewable Energy*, *225*, 120252. https://doi.org/10.1016/j.renene.2024.120252

Pippia, T., Sijs, J., & De Schutter, B. (2019). A single-level rule-based model predictive control approach for energy management of grid-connected microgrids. *IEEE Transactions on Control Systems Technology*, *28*(6), 2364-2376. https://doi.org/10.1109/TCST.2019.2945023

Purohit, I., Bose, S. K., & Atla, C. R. (2026). Techno-economics of grid connected Battery Energy Storage System (BESS) in power distribution: Case study of distribution company in India. Energy for Sustainable Development, 92, 101934. https://doi.org/10.1016/j.esd.2026.101934

Rana, A., & Gróf, G. (2024). Prosumer potential assessment and techno-economic feasibility analysis of rural electrification. Energy Conversion and Management: X, 22, 100542. https://doi.org/10.1016/j.ecmx.2024.100542

Rasoulzadeh-akhijahani, A., & Mohammadi-ivatloo, B. (2015). Short-term hydrothermal generation scheduling by a modified dynamic neighborhood learning based particle swarm optimization. *International Journal of Electrical Power & Energy Systems*, *67*, 350-367. https://doi.org/10.1016/j.ijepes.2014.12.011

Recalde, A., Cajo, R., Velasquez, W., & Alvarez-Alvarado, M. S. (2024). Machine Learning and Optimization in Energy Management Systems for Plug-In Hybrid Electric Vehicles: A Comprehensive Review. *Energies*, *17*(13), 3059. https://doi.org/10.3390/en17133059

Shadaei, M., & Samet, H. (2020, June). Using non-linear controller in peer-to-peer energy trading between distributed generations. In *2020 IEEE International Conference on Environment and Electrical Engineering and 2020 IEEE Industrial and Commercial Power Systems Europe (EEEIC/I&CPS Europe)* (pp. 1-5). IEEE. https://doi.org/10.1109/EEEIC/ICPSEurope49358.2020.9160508

Sharma, P., Saini, K. K., Mathur, H. D., & Mishra, P. (2024). Improved energy management strategy for prosumer buildings with renewable energy sources and battery energy storage systems. *Journal of Modern Power Systems and Clean Energy*, 12(2), 381-392. https://doi.org/10.35833/MPCE.2023.000761

Subramanian, V., & Bereznychenko, V. (2025). Cognitive fuzzy logic-integrated energy management for self-sustaining hybrid renewable microgrids. *Scientific Reports*, *15*(1), 1-17. https://doi.org/10.1038/s41598-025-94077-z

Vadi, S., Bildirici, M., & Kaplan, O. (2025). Performance Comparison of Metaheuristic and Hybrid Algorithms Used for Energy Cost Minimization in a Solar–Wind–Battery Microgrid. *Sustainability*, *17*(19), 8849. https://doi.org/10.3390/su17198849

Wang, J., Lyu, C., Bai, Y., Yang, K., Song, Z., & Meng, J. (2024). Optimal scheduling strategy for hybrid energy storage systems of battery and flywheel combined multi-stress battery degradation model. *Journal of Energy Storage*, 99, 113208. https://doi.org/10.1016/j.est.2024.113208

Wang, X., Mao, X., & Khodaei, H. (2021). A multi-objective home energy management system based on internet of things and optimization algorithms. *Journal of Building Engineering*, *33*, 101603. https://doi.org/10.1016/j.jobe.2020.101603

Wu, Y., Wu, Y., & Liu, X. (2019). Couple-based particle swarm optimization for short-term hydrothermal scheduling. *Applied Soft Computing*, *74*, 440-450. https://doi.org/10.1016/j.asoc.2018.10.041

Wynn, S. L. L., Boonraksa, T., Boonraksa, P., Pinthurat, W., & Marungsri, B. (2023). Decentralized Energy Management System in Microgrid Considering Uncertainty and Demand Response. *Electronics*, *12*(1), 237. https://doi.org/10.3390/electronics12010237

Yao, L., Yang, B., Cui, H., Zhuang, J., Ye, J., & Xue, J. (2016). Challenges and progresses of energy storage technology and its application in power systems. *Journal of Modern Power Systems and Clean Energy*, *4*(4), 519-528. https://doi.org/10.1007/s40565-016-0248-x

Yousri, D., Farag, H. E., Zeineldin, H., & El-Saadany, E. F. (2023). Integrated model for optimal energy management and demand response of microgrids considering hybrid hydrogen-battery storage systems. *Energy Conversion and Management*, *280*, 116809. https://doi.org/10.1016/j.enconman.2023.116809

Zafar, R., Mahmood, A., Razzaq, S., Ali, W., Naeem, U., & Shehzad, K. (2018). Prosumer based energy management and sharing in smart grid. *Renewable and Sustainable Energy Reviews*, *82*, 1675-1684. https://doi.org/10.1016/j.rser.2017.07.018

Zakeri, B., & Syri, S. (2015). Electrical energy storage systems: A comparative life cycle cost analysis. *Renew. Sustain. Energy Rev*, *42*(2015), 569-596. https://doi.org/10.1016/j.rser.2014.10.011

Zhang, C., Qiu, J., Yang, Y., & Zhao, J. (2021). Trading-oriented battery energy storage planning for distribution market. *International Journal of Electrical Power & Energy Systems*, *129*, 106848. https://doi.org/10.1016/j.ijepes.2021.106848

Zhou, H., Bi, J., Lv, Y., Zhao, W., Zhang, H., & Du, T. (2025). Techno-economic analysis of solar photovoltaic systems integrated with battery energy storage for university campuses. *Journal of Energy Storage*, *129*, 117360. https://doi.org/10.1016/j.est.2025.117360

Zhou, X., Xue, S., Du, H., & Ma, Z. (2023). Optimization of building demand flexibility using reinforcement learning and rule-based expert systems. *Applied Energy*, *350*, 121792. https://doi.org/10.1016/j.apenergy.2023.121792

© 2026. The Author(s). This article is an open access article distributed under the terms and conditions of the Creative Commons Attribution-ShareAlike 4.0 (CC BY-SA) International License (http://creativecommons.org/licenses/by-sa/4.0/)

Appendix A

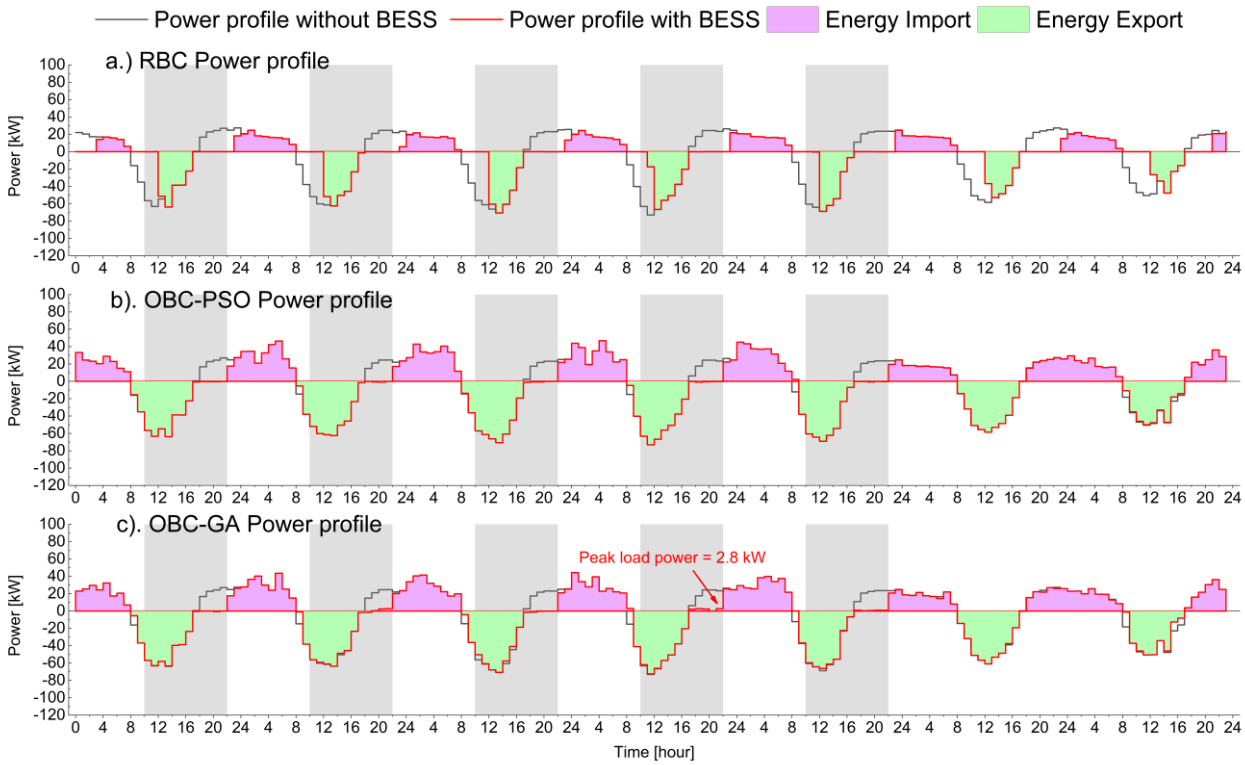


Fig A1. Weekly power profiles for the S5 prosumer during summer: Obtained energy import, export, and power profiles under using the (a) RBC, (b) OBC-PSO, and (c) OBC-GA strategies.

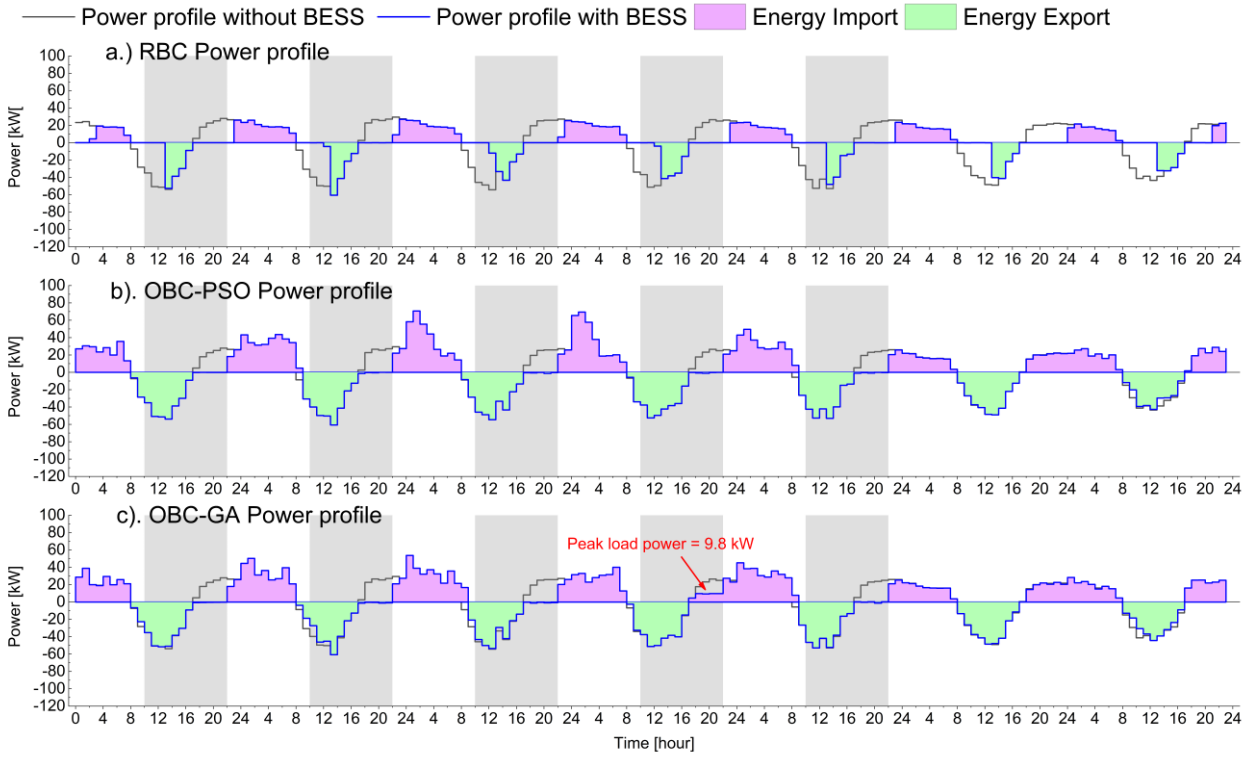


Fig A2. Weekly power profiles for the S5 prosumer during rainy season: Obtained energy import, export, and power profiles under using the (a) RBC, (b) OBC-PSO, and (c) OBC-GA strategies.

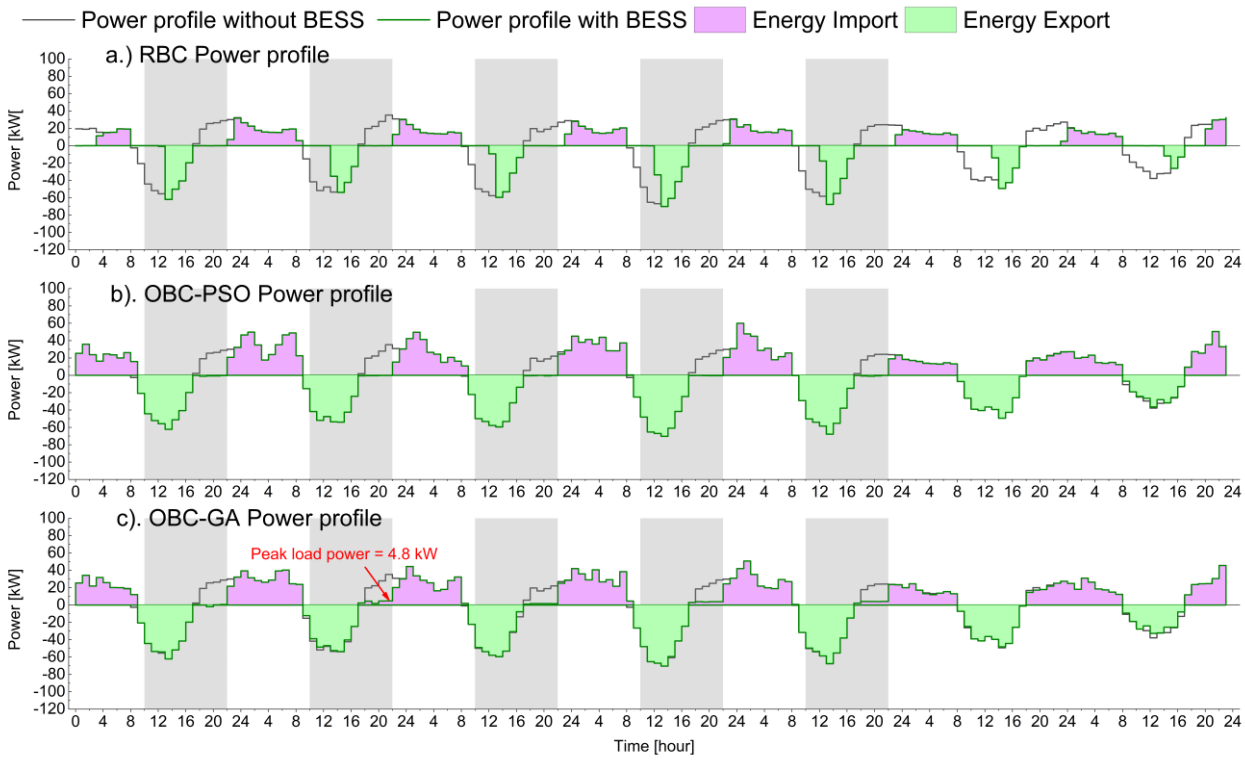


Fig A3. Weekly power profiles for the S5 prosumer during winter: Obtained energy import, export, and power profiles under using the (a) RBC, (b) OBC-PSO, and (c) OBC-GA strategies.